Zoological Journal of the Linnean Society, 2008, **152**, 717–736. With 10 figures

Morphology of the jaw system in trichiurids: trade-offs between mouth closing and biting performance

N. DE SCHEPPER[1]*, S. VAN WASSENBERGH[2] and D. ADRIAENS[1]

[1]*Ghent University, Evolutionary Morphology of Vertebrates, K.L. Ledeganckstraat 35, B-9000 Ghent, Belgium*
[2]*Universiteit Antwerpen, Laboratory for functional morphology, Universiteitsplein 1, B-2610 Wilrijk, Belgium*

Received 7 March 2007; accepted for publication 27 June 2007

In this study, we focus on two piscivore species of cutlassfishes (Trichiuridae) that show some degree of differences in morphology of the jaw system: *Aphanopus carbo* and *Trichiurus lepturus*. As studies dealing with myological features of *A. carbo* and *T. lepturus* are presently lacking, we first provide a detailed description of the head musculature of *A. carbo* and *T. lepturus*. Secondly, we focus on the mechanics of the mouth closing system of these trichiurids by using biomechanical modelling. More specifically, models allows us to: (1) describe the differences between how the lower jaw lever system works during mouth closure and during generating static bite force; (2) evaluate the effects of morphological change on the performance of both functions; (3) determine whether the configuration of each component of the lower jaw lever system is a compromise between both functions, or whether there is a partition of function (optimization for either hard biting or fast jaw closing) between the different parts of the jaw closing musculature; and (4) discuss the dynamical implications of having elongate jaws for capturing prey. © 2008 The Linnean Society of London, *Zoological Journal of the Linnean Society*, 2008, **152**, 717–736.

ADDITIONAL KEYWORDS: adductor mandibulae complex – bite force – elongate jaws – function – myology.

INTRODUCTION

A central goal in understanding evolutionary processes associated with species radiation is the recognition of conflicts in the performance of functions with high ecological significance (Barel, 1983). Two functions are conflicting when they require opposing biomechanical or physiological adaptations. In that case, both functions cannot be optimized in the course of evolution (Stearns, 1992). Consequently, trade-offs are often observed when certain components of the musculo-skeletal system have to participate in different functions (e.g. Losos, Walton & Bennett, 1993; Brainerd & Simons, 2000; Irschick, 2002; Pasi & Carrier, 2003; Schondube & Del Rio, 2003).

The head of fishes is one of the best examples of a complex and integrated system that has to accomplish several crucial biological functions (Liem, 1980): capturing, processing and transporting prey, breathing water or air, participating in sensory perceptions, providing protection for the major sense organs and brains, and serving as a streamlined bow in locomotion. In order to survive, fish must have an architectonic configuration of the head that specifically meets the structural and dynamical needs of each of these functions.

The lower jaw lever system of predatory fishes has to cope with two important performance traits: (1) quickly closing the mouth at the moment the prey is entering the mouth aperture or when the prey can be caught somewhere between the oral teeth; and (2) producing bite force in order to immobilize, crush or tear pieces from prey. However, previous modelling studies have shown that fast mouth closing and forceful biting have different morphological demands (Westneat, 1994, 2004; Turingan, Wainwright & Hensley, 1995; Collar, Near & Wainwright, 2005;

*Corresponding author. E-mail: natalie.deschepper@ugent.be

Kammerer, Grande & Westneat, 2005; Van Wassenbergh *et al*., 2005). As a result, it has been observed that fish hunting for evasive prey generally have a lever system of the lower jaw that appears to favour rapid closure of the mouth, while the jaws of fish preying on hard items are generally built to generate high bite forces at the cost of the speed at which the jaws can be moved (Westneat, 1994, 2004; Turingan *et al*., 1995; Collar *et al*., 2005; Kammerer *et al*., 2005).

From a biomechanical point of view, an intriguing situation occurs when prey capture performance depends equally on the maximal speed at which a fish can snap its jaws and on the maximal force its oral teeth can be pressed against or into the prey. This situation occurs in long-jawed fishes that have large, sharp teeth on the mandible, as in, for example, most Lepisosteidae, Bellonidae, Sphyraenidae or Trichiuridae. These fishes predominantly rely on piercing of the teeth into agile prey (Sibbing & Nagelkerke, 2001). How does the jaw system in these fishes deal with the trade-off between speed and force when it needs both to capture prey efficiently?

In this study, we focus on two piscivore species of cutlassfishes (Trichiuridae) that show some degree of differences in morphology of the jaw system: *Aphanopus carbo* and *Trichiurus lepturus*. As studies dealing with myological features of *A. carbo* and *T. lepturus* are presently lacking, we first provide a detailed description of the head musculature of *A. carbo* and *T. lepturus*. Secondly, we focus on the mechanics of the mouth closing system of these trichiurids by using biomechanical modelling. More specifically, models will allow us to: (1) describe the differences between how the lower jaw lever system works during mouth closure and when generating static bite force; (2) evaluate the effects of morphological change on the performance of both functions; (3) determine whether the configuration of each component of the lower jaw lever system is a compromise between both functions, or whether there is a partition of function (optimization for either hard biting or fast jaw closing) between the different parts of the jaw closing musculature (Friel & Wainwright, 1999); and (4) discuss the dynamical implications of having elongate jaws for capturing prey.

MATERIAL AND METHODS

SPECIES

Aphanopus carbo Lowe, 1839 is a remarkably elongate and laterally compressed species, found in the North Atlantic Ocean (Nakamura & Parin, 1993; Anon, 2000). This species is a benthopelagic predator but migrates to midwater during the night to feed. Their predatory life style, especially the fact that they span considerable depth differences when hunting, is even reflected in the modified and reinforced gas bladder (Bone, 1971; Howe, 1979). The diet mainly comprises crustaceans, cephalopods and fishes (mostly macrourids, morids, alepocephalids, *Micromesistius*, *Argentina*) (Swan, Gordon & Shimmield, 2003). Larger specimens tend to feed on larger prey (fish and cephalopods) and less on crustaceans (Costa, Chubb & Veltkamp, 2000).

Trichiurus lepturus Linnaeus, 1758, a cosmopolitan coastal species, is distributed throughout tropical and temperate waters between 60°N and 45°S (Martins & Haimovici, 1997; Kwok & Ni, 2000; Cheng *et al*., 2001). These benthopelagic, elongated fish are found in shallow coastal waters over muddy sand bottoms of the continental shelf. They are known to feed near the surface during daytime and migrate to the bottom during the night (Cheng *et al*., 2001). *T. lepturus* are predators, mainly feeding on large-sized pelagic and benthic fish (90.9%), crustaceans (10.9%) and cepalopods (2.5%) (Wojciechowski, 1972; Martins & Haimovici, 1997; Chiou *et al*., 2006). Food composition changes with size: small specimens predominantly feed on crustaceans, while large specimens mainly feed on fish and cephalopods (Wojciechowski, 1972).

The osteology and phylogeny of the cutlassfishes has been examined by Gago (1998). The most notable osteological difference between *A. carbo* and *T. lepturus* is found at the level of the supraoccipital. *T. lepturus* possesses an elevated supraoccipital crest, formed by the confluence of the frontal ridges, while in *A. carbo* the posterior confluence of the frontal ridges does not form a crest (Tucker, 1956; Gago, 1998). Additional, though small, cranial differences are observed in the length of the epiotics, pterotics and vomer (Gago, 1998). Although both species are popular subjects in studies focusing on phylogeny, diet, predation, distribution, abundances, movements, age and growth to determine stock dynamics (Pepin, Koslow & Pearre, 1988; Martins & Haimovici, 1997; Studholme *et al*., 1999; Figueiredo *et al*., 2003), morphological data concerning cranial myology are currently lacking and are therefore provided in detail in this study.

SPECIMENS

Five *Aphanopus carbo* specimens were commercially obtained from Madeira (Portugal). Three males and two females were examined, measuring between 111.3 and 124.7 cm standard length. Five specimens, three males and two females, of *Trichiurus lepturus* were obtained from the Museum of Comparative Zoology-Harvard (MCZ 58488), measuring between 83.2 and 100.1 cm standard length. Osteological features were

Table 1. Alphabetical list of abbreviations used in illustrations

$A_{1,\ 2,\ 3}$ Aω	Parts of the adductor mandibulae complex	PHβ	Superior part of protractor hyoidei
AAP	Adductor arcus palatini	Pr C Op	Caudal process of the opercle
AO	Adductor operculi	Pr D Op	Rostro-dorsal process of the opercle
BH	Basihyal	R Br	Branchiostegal rays
CH A	Anterior ceratohyal	r Hm	Elongate ridge of hyomandibula
CH P	Posterior ceratohyal	Scar A	Supracarinalis anterior
Cl	Cleithrum	SH	Sternohyoideus
D HH	Dorsal hypohyal	T A_1–A_2	Tendon of A_1–A_2
DO D	Dorsal part of dilatator operculi	T A_3	Tendon of A_3
DO V	Ventral part of dilatator operculi	T Aω	Tendon of Aω
Epax	Epaxial muscle	T Aω-IOp	Tendon of Aω to interopercle
Fa	Fascia	T Aω-Q	Tendon of Aω to quadrate
GL	Gill lamellae	T DO	Tendon of dilatator operculi
HH AB	Hyohyoideus abductor	T HH AB A	Anterior tendon of hyohyoideus abductor
HH AD	Hyohyoideus adductores	T HH AB P	Posterior tendon of hyohyoideus abductor
Hyp	Hypaxial muscles	T LAP	Tendon of levator arcus palatini
Incl D	Inclinatores dorsales	T LO	Tendon of levator operculi
Int	Intermandibularis	T Mx	Tendon of A_1–A_2 to maxillary
L BH-HH	Ligament between basihyal and dorsal hypohyal	T PH A	Common anterior tendon of PHβ and PHα
L prim	Primordial ligament	T PHα P	Posterior tendon of PHα
L UH-HH	Ligament between urohyal and dorsal hypohyal	T PHβ P	Posterior tendon of PHβ
LAP	Levator arcus palatini	T SB	Sternobranchial tendon
LO	Levator operculi	T sh	Tendinous sheet covering A_1–A_2
PHC E	Pharyngoclavicularis externus	T SH	Tendon of sternohyoideus
PHC I	Pharyngoclavicularis internus	V HH	Ventral hypohyal
PHα	Inferior part of protractor hyoidei	UH	Urohyal

examined using cleared and stained specimens according to the protocol of Hanken & Wassersug (1981). Osteological data of trichiurids were verified with published data of Gago (1998). The nomenclature of the skeletal elements follows Gago (1998). Myological data from these species were obtained by means of dissecting alcohol-preserved specimens using fibre staining (Bock & Shear, 1972). Terminology of myological features follows Winterbottom (1974). Drawings were made by use of a stereoscopic microscope (Olympus SZX-9), equipped with a camera lucida and a Colorview 8 digital camera. The illustrations and descriptions of the shape and structures of the muscles, as well as their positions are given with respect to the skeletal elements. Abbreviations used in this manuscript are given in Table 1.

Biometrics of the lower jaw lever system

In order to model the jaw-closing system of both species, a number of morphological variables were measured from preserved specimens (Fig. 1, Table 2). To do so, first the *xy* coordinates in the lateral view plane were determined for the lower jaw rotation point, the rostral tip of the lower jaw, and the insertion points on the lower jaw and the approximate origins on the neurocranium of each of the subdivisions of the adductor mandibulae complex (A_ω, A_1–A_2 and A_3). Secondly, the average pennation angle (θ) was estimated for each of these muscle bundles by measuring the angle between the central tendon of the muscle and muscle fibres at different locations across the muscle. Thirdly, the jaw adductors of both sides were removed and weighed. Next, the muscle bundles were immersed in a 30% HNO_3 solution for 24 h to dissolve the connective tissue. Fibres were gently teased apart and transferred to and stored in a 50% glycerol solution. Twenty muscle fibres per bundle were selected randomly and drawn using a Wild M5 dissecting microscope with a camera lucida, from which the average fibre length per bundle was determined. The physiological cross-sectional area (PCSA) of each bundle could then be calculated:

$$PCSA = \frac{muscle\ mass\ (\mathrm{g}) * \cos(\theta)}{\rho(\mathrm{g\,cm^{-3}}) * fibre\ length\ (\mathrm{cm})},$$

where θ is the average fibre pennation angle, and 1.0597 g cm^{-3} (Mendez & Keys, 1960) was used as an

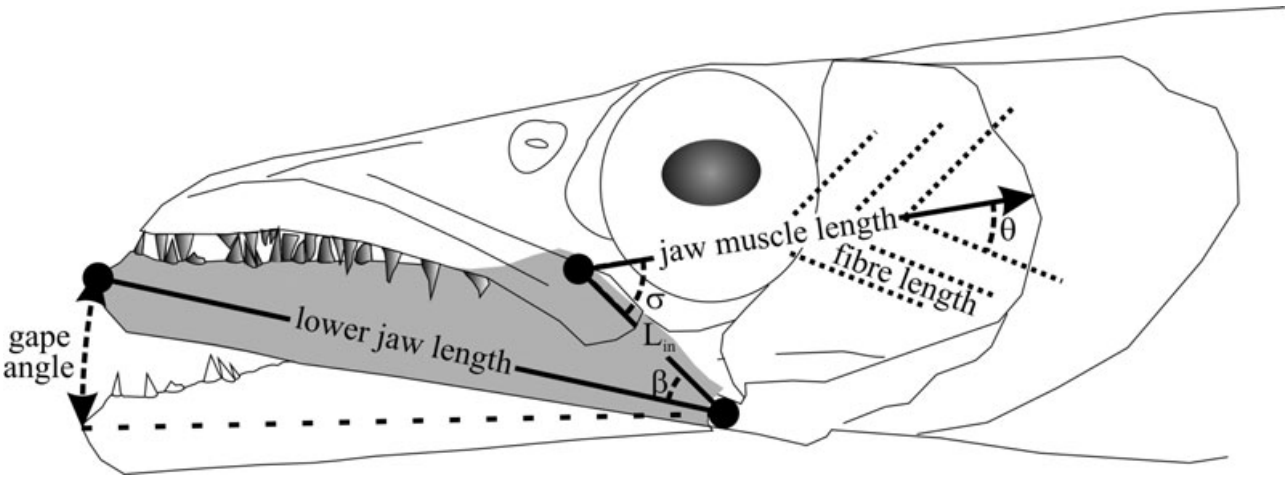

Figure 1. Schematic representation of the variables of the lower jaw lever system used for model calculations of bite force and mouth closing movements. β = angle between the lower jaw length axis and the input-lever (L_{in}), σ = angle between the input-lever (L_{in}) and the line of action of the jaw muscle, θ = average angle of pennation.

approximation for the density of the muscle tissue (ρ). Note that θ is a function of the instantaneous muscle length (Narici, 1999), and thus depends on gape angle. It is therefore assumed that the measured lengths from isolated muscle fibres (Table 2) correspond to the closed-mouth configuration of the jaw adductor muscles.

Model of mouth closing movements

Mouth closing movements were simulated using the model of Van Wassenbergh *et al*. (2005). This model calculates angular motion of the lower jaw based on the dynamic equilibrium of the external moments of force acting on the system. It has been shown to predict jaw-closing velocity of several morphologically different species of air-breathing catfishes (Clariidae) with reasonable accuracy. More specifically, there was generally less than 15% difference between experimentally observed data and the model's output for the time it takes to close the mouth (Van Wassenbergh *et al*., 2005). The model is therefore suitable to evaluate the effects of specific morphological changes to the jaw system of fishes, and to investigate in what aspects the jaw system is (or is not) optimized for fast mouth closing.

In this model, the lower jaw is modelled as a half-elliptic plate, the length and width of which correspond to the measured dimensions of the lower jaw measure for trichiurid species (Table 2). Upon rotation of this plate, a certain amount of water surrounding it will be put in motion as well. Therefore, the inertia of the rotating lower jaw is increased by including a virtual or added mass component that has the volume of the half-ellipsoid comprising the half-ellipse (Van Wassenbergh *et al*., 2005).

Upward rotation of the lower jaw is caused by contraction of the jaw adductor muscles. The model calculates the instantaneous angular acceleration ($\ddot{\alpha}$) of the lower jaw by using the following equation of motion:

$$I\,\ddot{\alpha} = M_m + M_d + M_{pr},$$

where I is the moment of inertia of the lower jaw and added mass with respect to the quadratomandibular axis of rotation, M_m, M_d and M_{pr} are the moments of force from, respectively, the jaw muscle activity, hydrodynamic drag, and a factor of resistance to jaw closing that combines the effects of the gradually increasing super-ambient pressure observed in the mouth cavity of suction-feeding fishes near the end of the jaw closing phase (Van Leeuwen & Muller, 1983) and the damping by elongation of the mouth-opening muscles and other tissues during mouth closing. For further information regarding estimates of the magnitude of each of these included factors during jaw closure, the reader is referred to the original publication of the model (Van Wassenbergh *et al*., 2005).

The instantaneous moment of force generated by the jaw muscles (M_m) is calculated by:

$$M_m = \sum F_m \sin(\sigma) L_{in},$$

where F_m is the instantaneous force along the line of action of one of the jaw muscle's subdivisions, and σ the instantaneous (gape-dependent) inclination of the jaw muscle with respect to the inlever with length L_{in}

Table 2. Biometric data of the closing system of the lower jaw

Species	Lower jaw length (mm)	Lower jaw width (mm)	Muscle	L_{in} (mm)	β (°)	Muscle length (mm)	σ (°)	*PCSA* (cm^2)	θ (°)	Avg. fibre length (mm)
T. lepturus	76.9	8.5	Aω	34.4	10	54.5	20	2.51	6	6.6
CL = 100.3 mm			A_1–A_2	24.0	26	45.9	52	0.99	32	17.5
			A_3	10.1	22	32.3	45	0.27	25	14.0
A. carbo										
CL = 160.6 mm	136.9	16.4	Aω	53.6	10	106.2	20	16.84	12	13.4
	(85.5)	(10.2)		(33.5)		(66.3)		(6.57)		(8.37)
			A_1–A_2	27.3	38	72.0	68	7.79	30	27.3
				(17.0)		(45.0)		(3.04)		(17.0)
			A_3	23.8	36	44.0	75	1.50	28	20.2
				(14.9)		(27.5)		(0.59)		(12.6)

CL = cranial length; L_{in} = inlever length; β = angle between the longitudinal axis of the lower jaw and L_{in}; σ = inclination of the line of action of the muscle with respect to L_{in}; PCSA = physiological cross-sectional area (both sides included); θ = average angle of pennation. For *A. carbo*, values scaled isometrically with respect to the CL of *T. lepturus* are shown beneath the measured values. All variables were measured in specimens with closed mouths (gape angle = 0°; see also Fig. 1).

(Fig. 1). The contractile properties determining the instantaneous force produced by the jaw muscle (F_m) are modelled as described in Van Wassenbergh *et al*. (2005). In this way, we accounted for the force–velocity dependence (Hill-curve), force–length dependence (optimal sarcomere overlap for a relevant range of gape angles), parallel elastic forces (elasticity in the muscle builds when it is stretched in a wide mouth opening) and included a sinusoidally rising activation profile (reaching full activation after 20 ms). In order to account for the force–length relationship, it was assumed that both species have optimal sarcomere overlap in each of their jaw muscles at a gape angle of 37°. In this way, there is favourable sarcomere overlap for a wide range of biomechanically relevant gape angles and the muscles do not reach the unstable, descending limb of the force–length curve when the mouth is opened to the maximal anatomical gape, which was estimated to be around 55° (manipulation of preserved specimens).

Calculation of bite force

Maximal bite force is calculated from the static equilibrium of forces at the tip of the lower jaw. In our calculations, maximal bite forces (F_{bite}) and the resultant prey reaction forces on the lower jaw tip are always perpendicular to the longitudinal axis of the lower jaw running from the centre of the quadratomandibular articulation to the tip of the lower jaw and are determined for different gape angles by:

$$F_{bite} = M_m / \textit{lower jaw length},$$

where M_m is the moment of force from the different jaw muscles in the isometric, fully activated state.

RESULTS

A detailed description of the head muscles of *A. carbo* is given below. To avoid repetition, only the myological differences observed in *T. lepturus* are mentioned.

Aphanopus carbo

Adductor mandibulae complex

The adductor mandibulae complex is a large muscle complex of the cheek region that covers the lateral surface of the suspensorium, below and behind the eye (Fig. 2A). Three main parts can be recognized: the adductor mandibulae A_1–A_2, separated from the A_3 (Fig. 3A) and the Aω (Fig. 4A).

1. The superficial part of the adductor mandibulae complex is referred to as A_1–A_2 since no clear-cut subdivisions (into the A_1 and A_2) are observed (Fig. 2A). Though based on the nomenclature of Winterbottom (1974) the presence of a tendinous

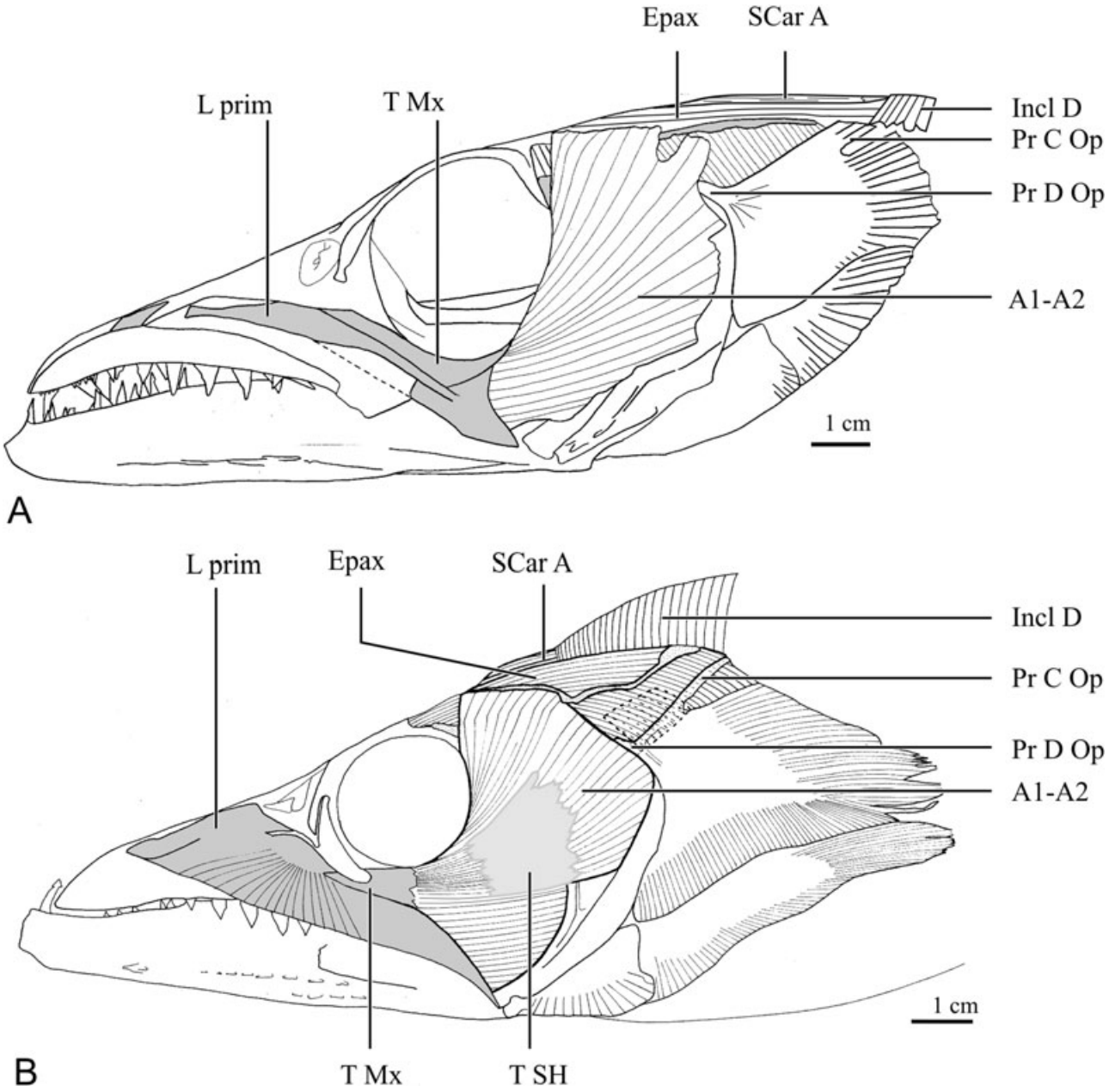

Figure 2. Lateral view of the cranial muscles of A, *Aphanopus carbo* and B, *Trichiurus lepturus*. Skin is removed. Dotted lines indicate parts of structures being covered by other elements. Tendons are illustrated in grey.

connection (T Mx) with the maxilla, lachrymal and primordial ligament suggests the presence of the A_1. The bulk of the fibres of this complex may represent the A_2 of the adductor mandibulae complex, according to the nomenclature of Winterbottom (1974) as they are latero-ventrally situated and insert indirectly onto the Meckelian fossa by means of the tendon T $A_1 - A_2$ (Fig. 4A). This tendon additionally merges with the tendon of Aω. Most of the fibres of the A_1–A_2 complex are antero-ventrally directed. Some fibres bordering the posterior edge of the orbit are more dorso-ventrally orientated. These fibres originate musculously from the lateral surface of the frontal and the antero-lateral surface of the sphenotic, and cover the levator arcus palatini and the anterior part of the dilatator operculi. The remaining fibres originate musculously from the lateral ridge of the elongate ventral arm of the hyomandibula (Fig. 3A), the anterior border of the preopercle, the antero-ventral part of the lateral

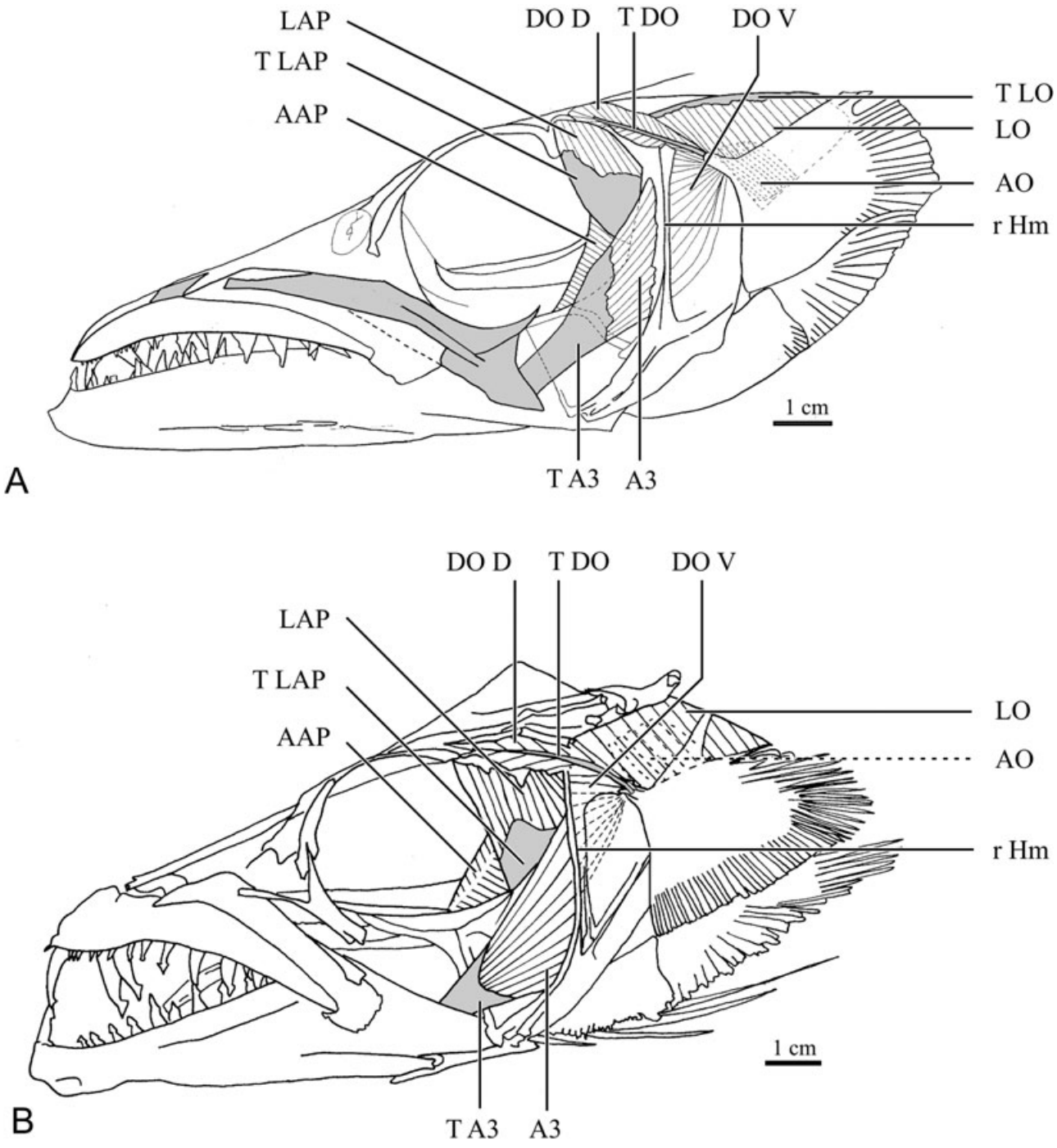

Figure 3. Lateral view of the cranial muscles of A, *Aphanopus carbo* and B, *Trichiurus lepturus*. A_1–A_2 of the adductor mandibulae complex is removed. Dotted lines indicate parts of structures being covered by other elements. Tendons are illustrated in grey.

surface of the quadrate and the antero-dorsal part of the metapterygoid.

2. The second part of the adductor mandibulae complex, the A_3, is the most medial part (Fig. 3A). The origin of the A_3 includes the ventral two-thirds of the crescentic anterior edge of the preopercle, the ventro-posterior part of the lateral surface of the metapterygoid, the lateral surface of the symplectic and the ventro-posterior part of the lateral surface of the quadrate. The tendon of

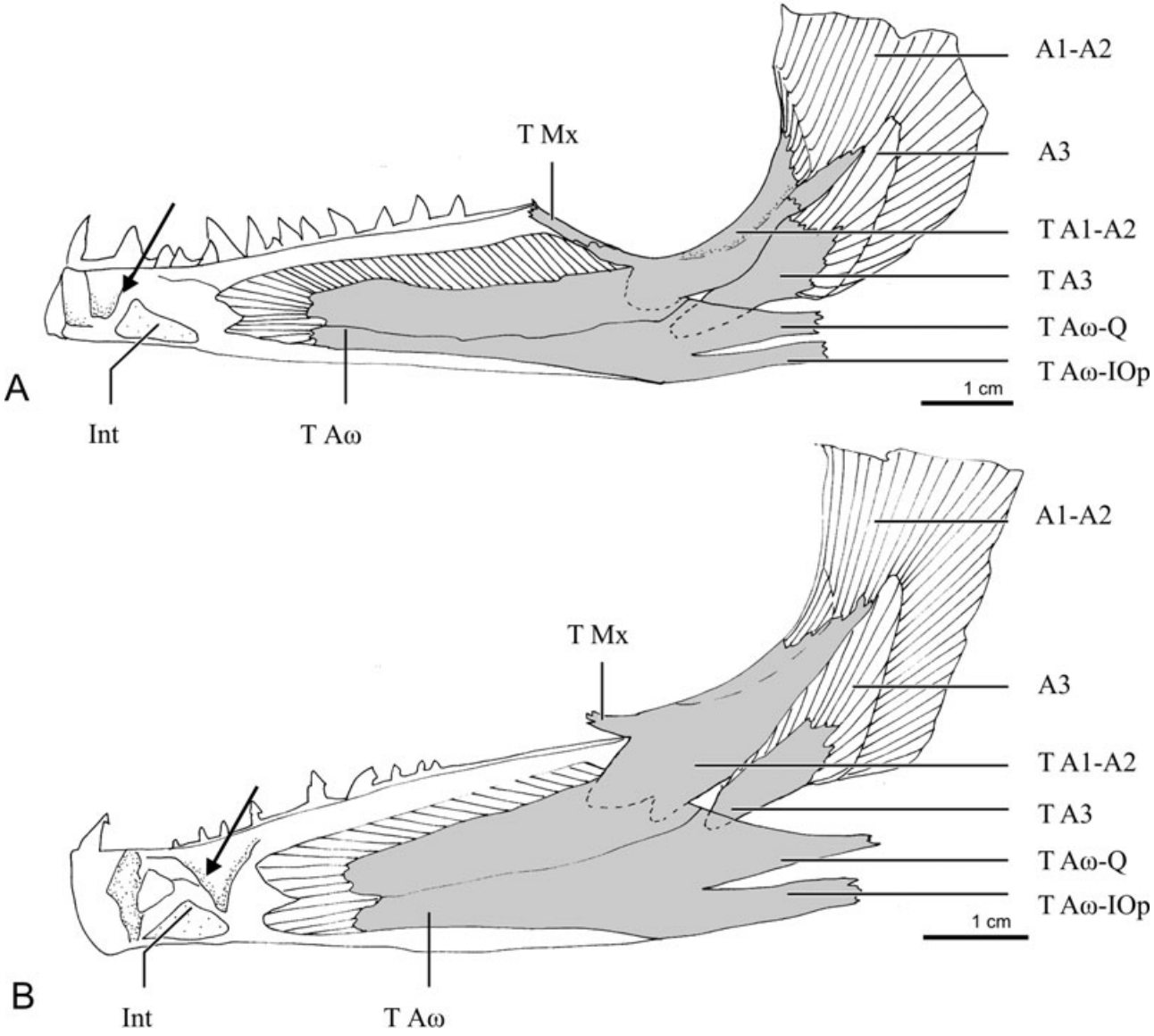

Figure 4. Medial view of lower jaw and adductor mandibulae complex of A, *Aphanopus carbo* and B, *Trichiurus lepturus*. Arrows indicate space in lower jaw in which fangs of upper jaw fit.

the A_3 inserts between the medial surface of the dentary and the lateral surface of the Aω, in the Meckelian fossa (Fig. 4A).

3. The third part and anterior expansion of the adductor mandibulae complex, Aω, consists of many short fibres which are antero-dorsally to antero-ventrally directed (Fig. 4A). The insertion site includes the medial surface of the dentary and is expanded by the presence of a longitudinal bony ridge. These fibres are connected to a broad and strong tendon T Aω, which fuses with the tendon of A_1–A_2 (Fig. 4A). Additionally, the T Aω splits postero-ventrally into two tendons: T Aω-Q attaches to the medial surface of the quadrate, near its caudal border, while T Aω-IOp attaches to the medio-lateral surface of the interopercle, near its rostral border.

Levator arcus palatini

The levator arcus palatini is a triangular muscle, with postero-ventrally orientated fibres (Fig. 3A). This muscle stretches from its origin, being the frontal, pterosphenoid and sphenotic to a rather large insertion surface, i.e. the dorsal two-thirds of the dorso-lateral surface of the metapterygoid and the dorso-anterior edge of the hyomandibula. The insertion is accomplished by means of a superficial,

flat tendon. The posterior fibres are incompletely separated from the anterior fibres of the dilatator operculi.

Adductor arcus palatini
This muscle is situated in the roof of the buccal cavity and extends between the skull and the suspensorium, forming the posterior and postero-ventral margin of the orbit (Fig. 3A). The postero-dorsal half of the adductor arcus palatini is covered by the levator arcus palatini. The rostral half of the muscle is relatively thin and becomes gradually thicker posteriorly. The fibres are latero-ventrally directed and originate from the parasphenoid and prootic. They insert musculously as a narrow strip on the medial surface of the metapterygoid and antero-medial edge of the hyomandibula.

Levator operculi
The levator operculi runs between the lateral skull wall and the opercle (Fig. 3A). Its anterior fibres are confluent with the posterior fibres of the dilatator operculi. The levator operculi arises from the neurocranium at the level of the pterotic and epiotic by means of a tendon sheet along the dorsal edge of the levator operculi over its total length (Fig. 3A). The latero-ventrally orientated fibres insert musculously on the dorso-medial surface of the opercle and on the medial surface of the opercle at the level of a medial ridge.

Adductor operculi
The adductor operculi is laterally covered by the anterior part of the levator operculi (Fig. 3A). The fibres arise musculously from the ventro-lateral surface of the pterotic and partially from the prootic. They insert on the medial surface of the opercle. The fibres run postero-ventrally and are laterally inclined.

Dilatator operculi
The dilatator operculi is subdivided into two parts: a dorsal and a ventral part. The dorsal part is long and slender and situated in the dilatator fossa (Fig. 3A). Its origin is extensive and includes the frontal, pterosphenoid, sphenotic, pterotic, hyomandibula and supratemporal. The anterior fibres form a bipennate muscle with a long tendon, which is clearly visible, inserting on the lateral plate-like process on the articular head of the opercle. Some posterior fibres of the dorsal part insert musculously on the lateral plate-like process of the articular head of the opercle as well. These fibres merge ventrally with the dorsal fibres of the second part. This second, ventral part of the dilatator operculi arises from the posterior edge of the hyomandibula and the medial surface of the preopercle. These fibres converge postero-dorsally to insert musculously on the latero-ventral side of the same lateral plate-like process on the articular head of the opercle.

Intermandibularis
The fibres of the intermandibularis stretches out transversally between the two halves of the dentary and lie caudal to the dental symphyse (Figs 4A, 5A).

Protractor hyoidei
The protractor hyoidei interconnects the hyoid with the dentary (Fig. 5A). The protractor hyoidei comprises two parts, an inferior α- and a smaller superior β-part. The two halves of the PHβ form two distinct bundles, separated by a deep, longitudinal groove containing the basihyal. The left and right halves of the PHα are ventro-medially fused. The PHβ is ventrally fused to the PHα. The anterior tendon of the PHβ is anteriorly fused with that of PHα, forming the anterior common tendon T PH A. This tendon inserts onto the dentary, just behind the intermandibularis. Posteriorly, the protractor hyoidei originates from the lateral surface of the anterior ceratohyal. The posterior tendons of the left and right PHβ run backwards to attach on the dorso-lateral surface of the anterior ceratohyal. The left and right halves of the PHα share a common posterior tendon. This common tendon splits posteriorly and each branch runs towards the ventro-lateral surface of, respectively, the left and right anterior ceratohyal. The posterior tendons of PHα and PHβ are connected by a tendinous sheet, which covers the antero-lateral surface of the anterior ceratohyal.

Hyohyoideus abductor
The hyohyoideus abductor connects the dorsal hypohyal to the first branchiostegal ray of each side (Fig. 6A). The anterior fibres of the hyohyoideus abductor originate through a broad, flat tendon from the ventro-lateral surface of the ventral hypohyal. The two robust urohyal–hypohyal ligaments are partially covered by these tendons. The posterior fibres of the hyohyoideus abductor of each side insert through a flat tendon on the anterior surface of the first branchiostegal ray of the opposite side. Both tendons of the left and right side thus cross each other in the midline.

Hyohyoidei adductores
Hyohyoidei adductores lie between the successive branchiostegal rays (Fig. 6A). Lateral fibres pass between the successive rays while the medial fibres form a continuous sheet on the medial side of the

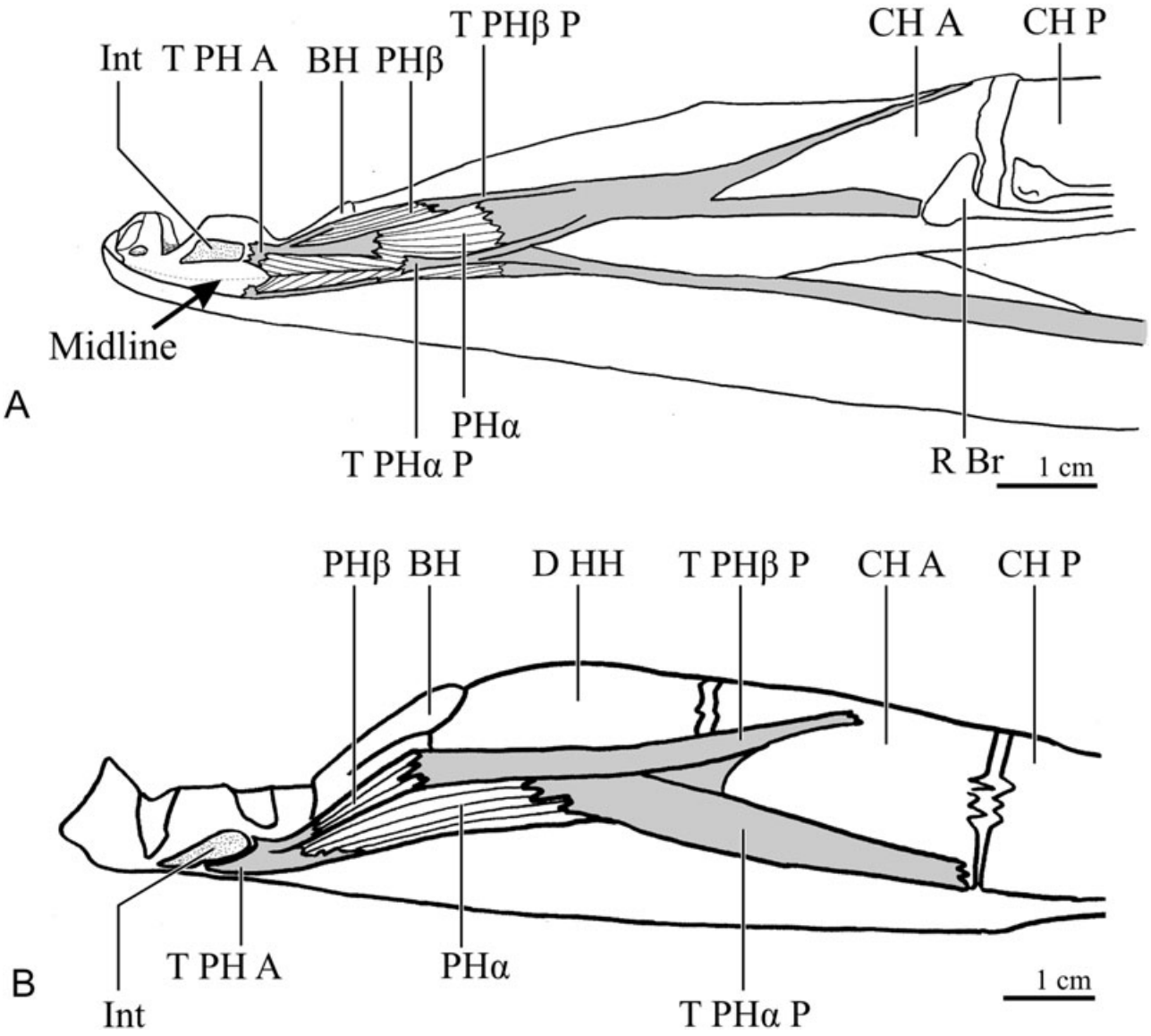

Figure 5. Lateral view of ventral muscles; antero-medial surface of lower jaw and medial surface of ceratohyals are visible; right lower jaw and right halve of the hyoid arch are removed. A, *Aphanopus carbo*. Lower jaw is slightly turned over to the right, partially visualizing the ventral surface. Ventral midline is indicated by arrow. B, *Trichiurus lepturus*.

branchiostegal rays and continue behind the postero-dorsalmost branchiostegal ray to attach to the medial surface of the opercle.

Sternohyoideus

Two myocommata divide the sternohyoideus into three myomeres (Fig. 7A). The two halves of the sternohyoideus are separated in the midline by an aponeurosis. The postero-dorsal fibres of the sternohyoideus originate from the lateral, anterior and medial surface of the cleithrum. The origin onto the cleithrum is postero-dorsally extended, dorsal to the origin of the pharyngoclavicularis internus. The pharyngoclavicularis externus and internus cover the sternohyoideal fibres, both originating from the lateral surface of the cleithrum. The postero-ventral fibres of the sternohyoideus are continuous with fibres of the hypaxialis and are laterally covered by a fascia. The anterior fibres of the muscle insert musculously and tendinously through the sternohyoideal tendon on the lateral surface of the urohyal. The antero-dorsally directed sternobranchial tendon is merged with the aponeurosis between the two halves of the sternohyoideus. Only the tip of this

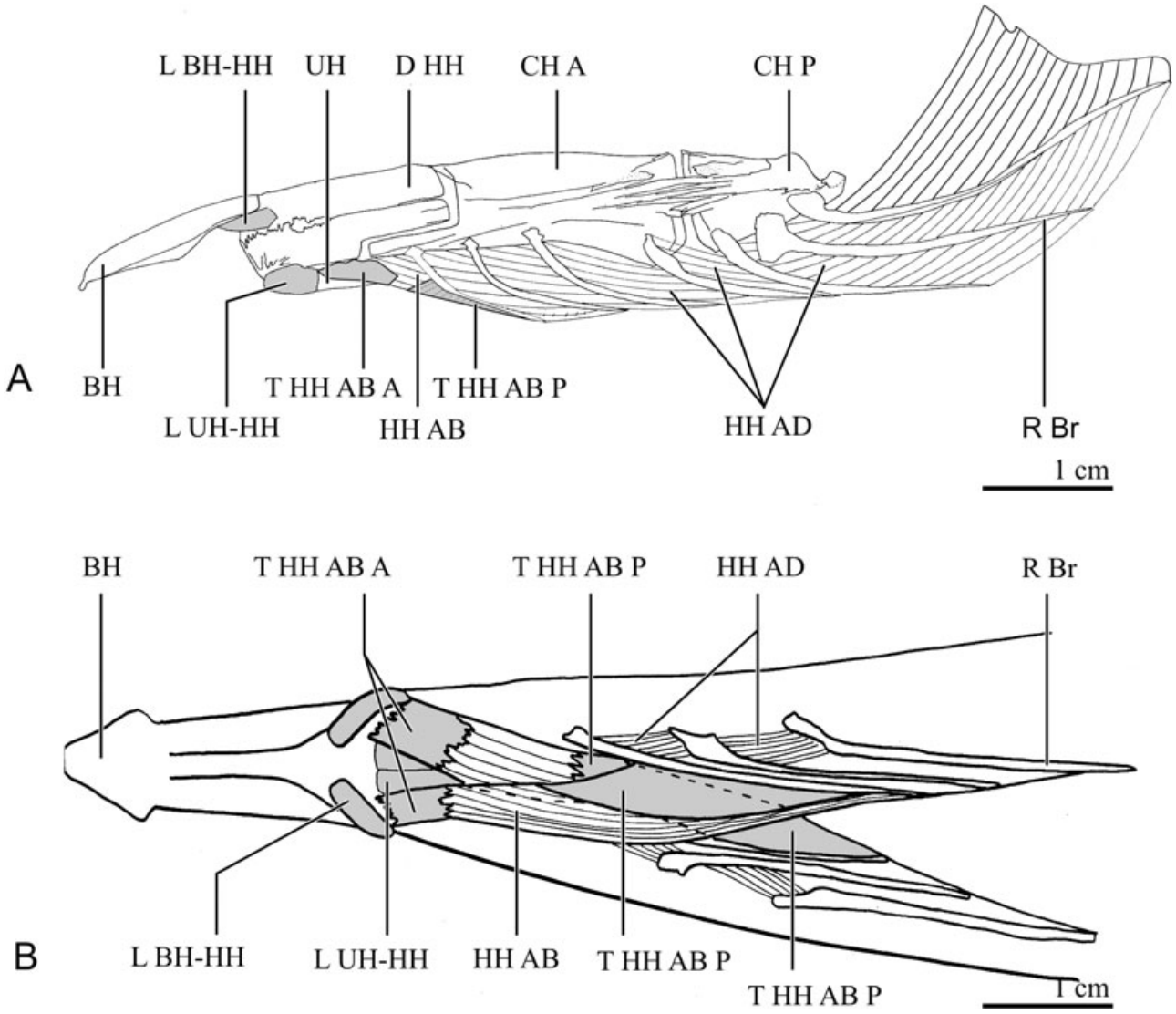

Figure 6. Hyohyoideus muscle complex. A, lateral view of hyohyoideus muscles in *Aphanopus carbo*; B, ventral view of hyohyoideus muscles in *Trichiurus lepturus*. Only the anterior bundles of the hyohyoidei adductores are drawn; the posterior fibres also interconnect the successive branchiostegal rays and finally run to the medial side of the opercle as is the case in *A. carbo*.

tendon lies superficially, and runs forward to attach to the ventral processus of the third hypobranchial element, after fusion with the tendon of the opposite side.

Pharyngoclavicularis internus

This muscle lies medial and posterior to the pharyngoclavicularis externus (Fig. 7A). It is tendinous at both its origin and its insertion. The posterior fibres attach tendinously to a small groove in the antero-lateral margin of the cleithrum. The fibres run in dorso-rostral direction. The anterior tendon inserts on the antero-ventral region of the fifth ceratobranchial.

Pharyngoclavicularis externus

This muscle originates from a groove on the antero-lateral surface of the cleithrum and inserts beneath a dorsal ridge on the dorso-mesial surface of the fifth ceratobranchial (Fig. 7A). The fibres run dorsally and slightly rostrally.

Epaxials

The epaxials originate from the dorsal surface of the neurocranium, above the posterior edge of the eye (Fig. 2A). The origin includes the frontals, parietals, exoccipitals, supraoccipital and epiotics. The origin is not additionally extended by a supraoccipital ridge.

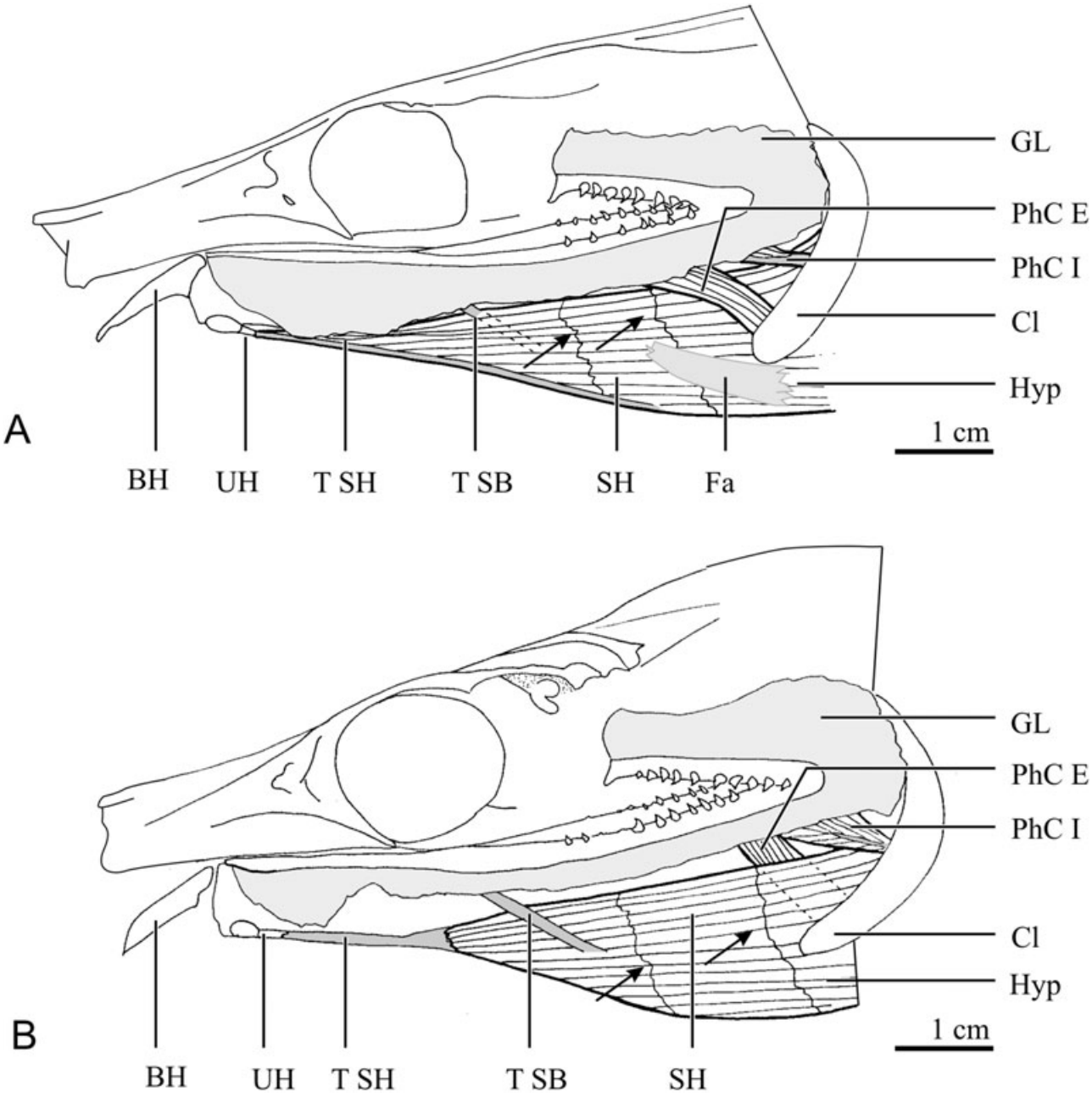

Figure 7. Lateral view of the sternohyoideus. Lower jaws, upper jaws and cranial muscles are removed, gill lamellae (pale grey) are partially cut and tendons are indicated in dark grey. Arrows show myocommata. A, *Aphanopus carbo*; B, *Trichiurus lepturus*.

Supracarinalis anterior

The anterior fibres of the supracarinalis anterior insert musculously on the postero-dorsal region of the skull, forming a cord-like muscle bundle in the dorsal midline (Fig. 2A). The posterior fibres originate by means of two postero-lateral tendons on the first pterygiophore of the dorsal fin. The fibres are antero-posteriorly directed.

MYOLOGICAL DIFFERENCES FOUND IN *TRICHIURUS LEPTURUS*

The cranial muscles in *T. lepturus* are very similar to those in *A. carbo* (Figs 2B-7B). Origin, insertion and configuration are similar in the levator arcus palatini, adductor arcus palatini, adductor operculi, dilatator operculi, intermandibularis, hyohyoidei abductores,

hyohyoidei adductores, pharyngoclavicularis internus and pharyngoclavicularis externus.

Adductor mandibulae complex
In *T. lepturus* the configuration of the adductor mandibulae complex is similar, though small differences are observed (Figs 2B, 3B). Some fibres arising from the dorsal half of the lateral surface of the preopercle seem to be somewhat separate from the body of the muscle mass, but are strongly connected by a superficial sheet of faint tendons, which is absent in *A. carbo*. The tendon T A_1–A_2 splits, in contrast to that in *A. carbo*, into two smaller parts which separately insert onto the edge of the dentary (Fig. 4B).

Levator operculi
The origin includes similar sites as in *A. carbo* though in *T. lepturus* the fibres arise musculously from the neurocranium (Fig. 3A). The tendon is absent.

Protractor hyoidei
As in *A. carbo*, both halves of the PHα are ventromedially fused (Fig. 5B). By contrast, in *T. lepturus* the fibres of the anterior tendons of the PHα halves are fused, forming one common ventral tendon which extends rostrally to insert on the dentary behind the intermandibularis. In contrast to *A. carbo*, the posterior tendons of the PHα remain separate in *T. lepturus*, whereas in *A. carbo* the posterior tendons of PHα are rostrally fused.

Sternohyoideus
The sternohyoideal tendon is shorter and situated in the anterior part of the muscle (Fig. 7B). The origin of the sternohyoideus includes the medial, anterior and lateral surface of the cleithrum. The origin of the pharyngoclavicularis externus is similar though its lateral surface is covered by a thin sheet of fibres of the sternohyoideus, inserting onto the cleithrum as well. The postero-ventral fibres of the sternohyoideus, also continuous with the hypaxials, are not laterally covered by a fascia. The sternobranchial tendon has a more superficial position (visible on the lateral surface of the sternohyoideus) compared with that in *A. carbo*. At about two-thirds of the length of the muscle this tendon becomes superficial.

Epaxials
Origin, insertion and configuration are similar, although the origin is expanded due to the presence of the supraoccipital ridge (Fig. 2B).

Supracarinalis anterior
The supracarinalis muscle is present in *T. lepturus* but due to the anterior displacement of the dorsal fin, compared with *A. carbo*, this muscle is less anterocaudally extended (Fig. 2B).

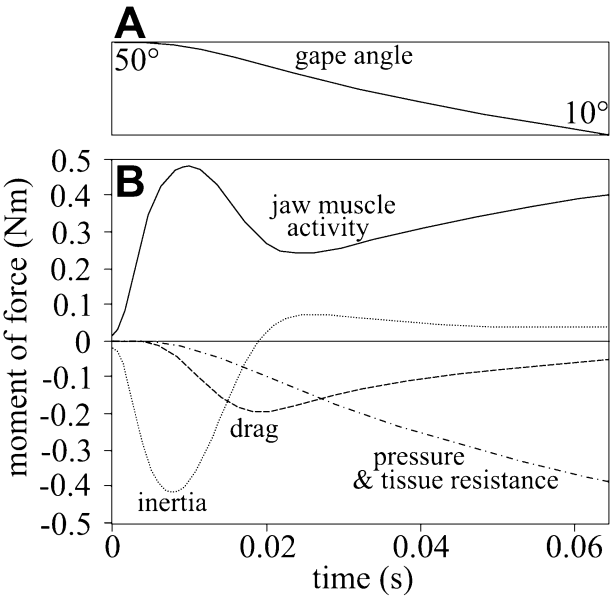

Figure 8. Model output of the moments of force (B) involved during a simulation of a mouth closure in *A. carbo* (cranial length of 160.6 mm) from a gape angle of 50° to 10° (A). Positive moments contribute to mouth closure, while negative moments work against mouth closure. The final lower jaw angle of 10° represents the moment of impact on a prey item. See text for further explanation.

Dynamics of mouth closing

The simulations with the mouth-closing model of *A. carbo* and *T. lepturus* show the following general pattern. Initially, during the first 15 ms after the start of mouth closing, jaw muscle force is almost entirely used to accelerate the lower jaw (Fig. 8). Shortly after this, when the lower jaw has nearly reached its maximal velocity (peak near 20 ms), drag becomes the most important factor of resistance to lower jaw rotation. During the final half of the mouth-closing phase (around 30–65 ms), the force generated by the jaw adductors is predominantly countering resistance caused by stretching of the jaw-opener muscles and the forces exerted on the lower jaw resulting from super-ambient pressure inside the mouth that typically appears near the end of mouth-closing (Fig. 8). According to the model, *A. carbo* is able to close its mouth from a gape angle of 50° to 10° in 64.8 ms, while *T. lepturus* needs 74.2 ms to achieve this.

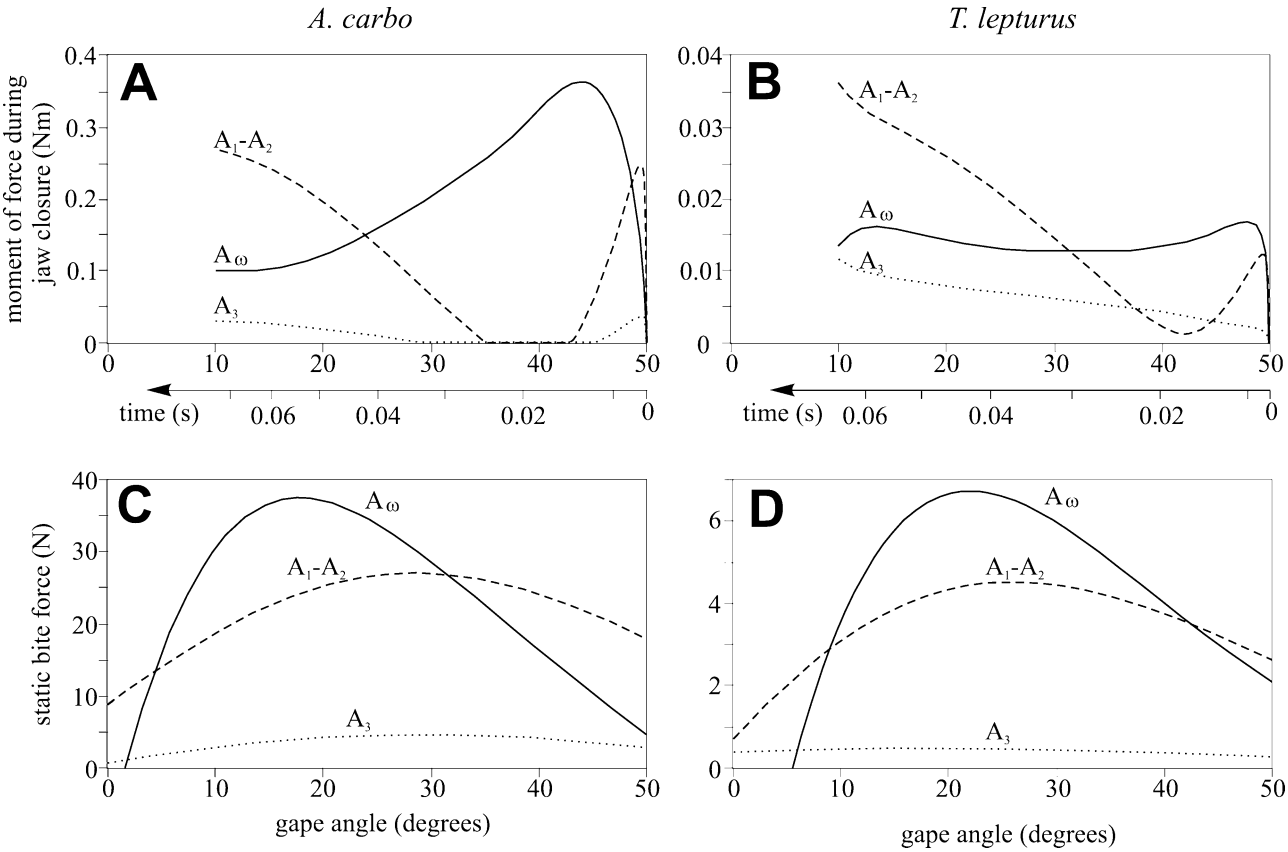

Figure 9. Model output of moment of force (A, B) during a lower jaw adduction from a gape angle of 50° to 10°, and maximal static bite force at the tip of (and perpendicular to) the lower jaw as a function of gape angle (C, D) produced by each of the subdivisions of the adductor mandibulae complex (Aω, A_1–A_2, A_3). Note that the higher moments and forces generated by *A. carbo* (left) with respect to *T. lepturus* (right) are partly due to its larger size (cranial lengths of 160.6 mm vs. 100.3 for *T. lepturus*), and partly because of the relatively larger cross-sectional area of the jaw muscles (Table 2). Further information is given in the text.

Function of the different jaw muscles during jaw closing and biting

The musculus adductor mandibulae consists of three subdivisions (Aω, A_1–A_2, A_3). The jaw muscle part with the highest PCSA, the Aω, is also the longest muscle (Table 2). It attaches to the lower jaw at a relatively low and distant position from the quadrato-mandibular joint. It consists of a large number of relatively short fibres. The PSCA of the A_1–A_2 subdivision is only 46.3 and 39.4% of that of the Aω for, respectively, *A. carbo* and *T. lepturus* (Table 2). It attaches higher on the lower jaw compared with the Aω, close to the coronoid process.

The insertion, inclination and pennation of the slenderest muscle part, the A_3, resemble closely those of the A_1–A_2, but its PCSA, muscle length and fibre length are considerably lower (Table 2).

According to dynamic and static modelling, the individual adductor mandibulae subdivisions differ notably in function during mouth closing and biting (Fig. 9). At the onset of jaw closing, each of the jaw muscle parts generates a considerable moment of force to accelerate the lower jaw rotation, with magnitudes roughly relative to their PSCA (Fig. 9A, B). Shortly thereafter, the total moment of force produced by the A_1–A_2, and also the A_3 in *A. carbo*, drops entirely and the Aω becomes dominant in powering mouth closure, being able to generate its highest mouth-closing torques during this period (Fig. 9A, B). Toward the end of mouth closure, the A_1–A_2 again becomes increasingly important, ultimately even doubling the amount of moment of force the Aω is able to produce at this instant, despite the larger PCSA of the latter muscle (Fig. 9A, B). The contribution of the slender A_3 in causing lower jaw adduction gradually increases as mouth closing goes on in *T. lepturus*, or similarly, recovers progressively in the second half of mouth closure in *A. carbo* (Fig. 9A, B)

Maximal bite force is produced at a gape angle of 20.2° in *A. carbo* and 26.0° in *T. lepturus*. More than 90% of this maximum bite force can be exerted on prey at gape angles between 13.2° and 30.2° for *A. carbo* and 19.1° and 35.5° for *T. lepturus*. According to the model, the Aω in both species is unable to produce force optimally for a wide range of gape angles, because of the force–length relationship. Because of its geometrical configuration within the jaw system (Table 2), the Aω is elongated considerably when the mouth is opened to a 50° gape angle. As a consequence, the muscle is predicted to lose substantial tension at short muscle lengths, when gape angles are narrow (Fig. 9C, D). The A_1–A_2 and A_3 subdivisions are able to generate bite force at a much wider range of gape angles compared with the Aω.

Effects of morphological change on biting and jaw closing performance

A trade-off between mouth-closing and biting performance is demonstrated by model simulations for three morphological variables: (1) the effects of changes in the length of the input lever arm for jaw closing (Fig. 10A); (2) the effects of changes in the length and cross-sectional area of the muscle, meaning that the total volume of the jaw muscle is kept constant (Fig. 10B); and (3) the effects of an increased or decreased inclination of the jaw muscle (Fig. 10C). The results show that the morphology of the jaw system of *A. carbo* and *T. lepturus* is neither optimal for generating high bite forces nor optimal for minimizing the time to close the mouth. The functional trade-off appears from the result that, in general, morphological change has the opposite effect on both functions: if bite performance is enhanced, then mouth-closing performance is reduced and vice versa (Fig. 10).

Some exceptions are observed for which the optimal configuration in a certain aspect of the jaw system is indicated for jaw-closing performance, but not for biting. First, jaw-closing performance could not be improved in any way by changing the input lever length, the jaw muscle shape or the inclination of the jaw muscle of the A_3 of *T. lepturus* (Fig. 10A2, B2, C2), indicating that this design is close to optimal for this function. A second noteworthy example is that there is very little room to increase the input-lever length of the Aω or to decrease the inclination of this muscle in both species and still be able to close the mouth from a gape angle of 50°. When implementing these morphological changes in the model, the line of action of Aω soon crosses the rotational axis of the lower jaw, through which the muscle will open instead of close the mouth upon activation. As a consequence, the geometrical configuration of the Aω in the jaw system is close to its limits for allowing a mouth opening of 50°. Given that interference with the capacity of opening the mouth widely is probably not favourable for the animal's feeding performance, the muscle is performing very close to its optimum for fast mouth closing (Fig. 10A, C).

DISCUSSION

Morphology

The morphology, origin and insertion of the cranial muscles are very similar in *T. lepturus* and *A. carbo*. Differences are found in the insertion of the epaxials and supracarinalis muscles. These differences are presumably related to the difference in cranial shape at the level of the supraoccipital crest (Fig. 2). In *T. lepturus* a heigher supraoccipital crest is formed by the confluence of the frontal ridges, while in *A. carbo* the posterior confluence of the frontal ridges does not form a crest (Tucker, 1956; Gago, 1998). The supraoccipital is known to serve as insertion site for the epaxials. Expanded insertion sites and increased input lever for the epaxials (by the presence of a crest) may have an effect on the functionality or efficiency of these dorsal body muscles (Liem & Osse, 1975; Bone, Marshall & Blaxter, 1995; Caroll *et al*., 2004). The differences in supracarinalis anterior muscles between both species are likely to be related to the anterior position of the dorsal fin in *T. lepturus*. The shape and size of the dilatator operculi is aberrant compared with that of most teleosts. In *T. lepturus* and *A. carbo*, this muscle comprises two parts and its origin is extended to the posterior edge of the hyomandibula and the medial surface of the preopercle. Although this configuration is unusual, fibres originating from the preopercle are observed in a few teleosts (e.g. *Cyclepus*, *Helostoma*; Winterbottom, 1974).

Functional morphology

An important goal in functional morphology is to identify how the mechanical design allows animals to perform in different functions that are essential but that require trade-offs with each other. The mathematical modelling in the present study showed that the morphology of the jaw-closing system in *Aphanopus carbo* and *Trichiurus lepturus* indeed displays a compromise in the performance to produce a powerful bite force and the ability to swing the lower jaw towards the upper jaw as quickly as possible (Fig. 10).

This result, however, is not surprising as trade-offs between maximization of force and velocity transfer in mouth closing systems have been suggested before and are found to be manifested in the natural diets of terrestrial vertebrates such as salamanders (Adams

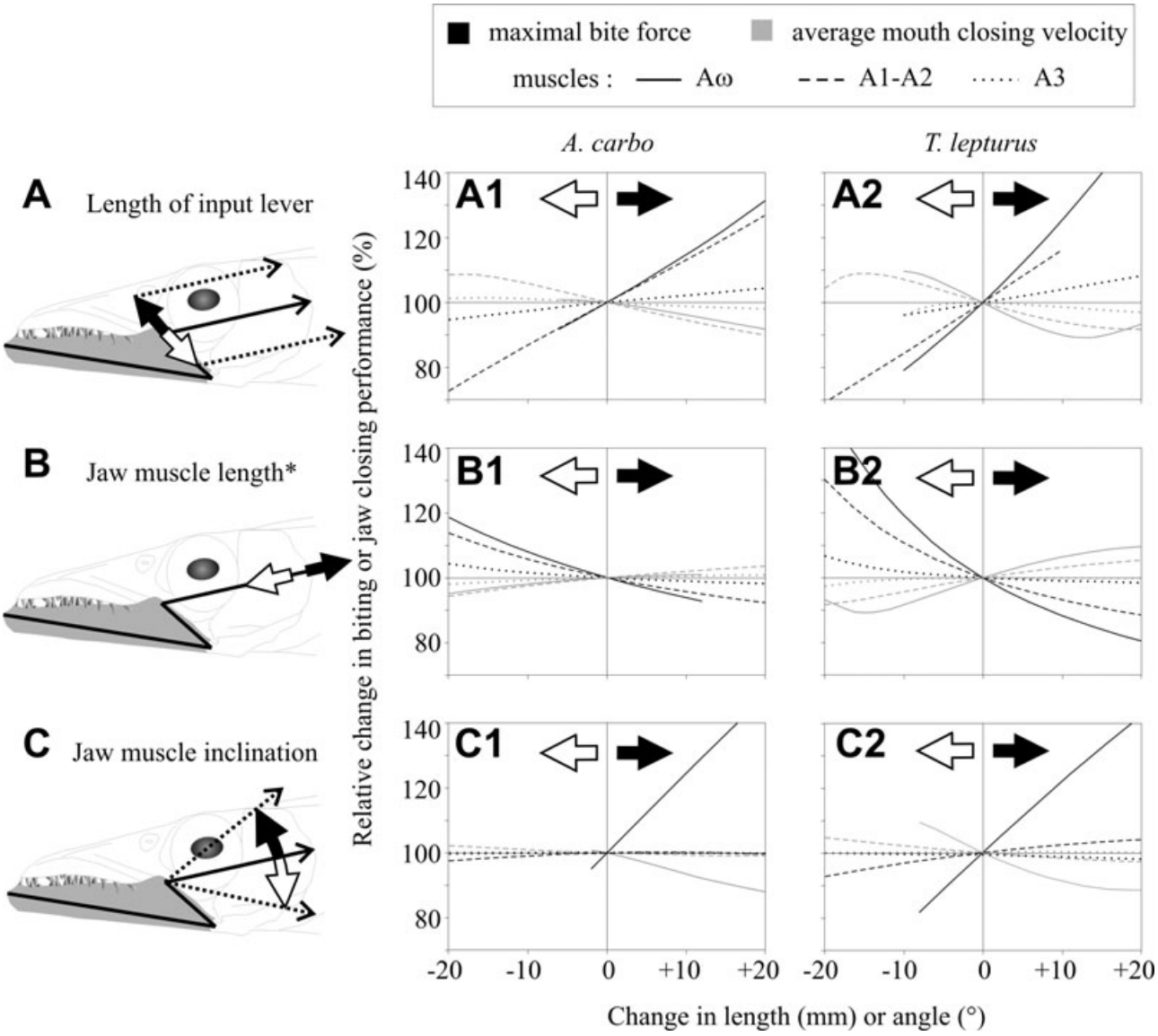

Figure 10. Effects of specific morphological changes to the jaw system (schematically illustrated in A, B, C; left column) on biting and mouth closing (50–10° gape) performance as calculated by the model for *A. carbo* (cranial length of 160.6 mm) and *T. lepturus* (cranial length of 100.3 mm). The measured configuration of the jaw system of each species corresponds to the central point in the graphs where all curves intersect (0 mm or 0°; 100%). Each morphological change was implemented for each muscle separately (see top for legend), while the model simulations were run with simultaneous activation of all muscles. In this way, the relative importance of modifications to each muscle is also displayed on the graphs. Note that, with few exceptions (see text for further information), increasing biting and mouth closing performance require morphological changes in the opposite direction. This demonstrates the functional trade-off between the two functions, and illustrates that the jaw system of both trichiurid species is a compromise between forceful biting and rapid snapping of the jaws. As expected from the relative contribution of each of the adductor mandibulae subdivisions to jaw-closing power (Fig. 9A, B) and bite force (Fig. 9C, D), changes to the Aω generally have the largest impact on jaw closing and biting performance, while changes to the A_3 have the smallest effects on the overall performances. The asterisk denotes that muscle volume was kept constant by adjusting the physiological cross-sectional area.

& Rohlf, 2000) and of fish species (Westneat, 1994, 2004; Turingan *et al*., 1995; Collar *et al*., 2005; Kammerer *et al*., 2005; Van Wassenbergh *et al*., 2005). Piscivores generally require the rapid capture of evasive prey and therefore benefit by favouring fast mouth closure. By contrast, animals relying on static biting to eat hard prey will favour the capacity to transfer force to the jaws, by which they inevitably

reduce their performance to close the mouth rapidly. However, this still leaves the question of how the complex jaw system, with the different parts of the jaw-adducting musculature (Fig. 2), is built for performing both functions sufficiently well in the examined trichiurid species, which need a quickly moving as well as a forceful jaw to pierce their teeth into elusive prey such as fish.

Elongate jaws

An important aspect of a predator's prey capture success, especially when feeding on elusive prey, is rapid mouth closure. The chance of prey escape may be reduced significantly by closing the mouth rapidly. Trichiurids mainly feed on large fish, which are usually fast and agile prey, and additionally on harder or tougher prey, e.g. cephalopods and crustaceans. Therefore, rapid snapping of the jaws onto prey can be important to reduce the chance of prey escape, and a powerful bite is required as well (Wojciechowski, 1972; Martins & Haimovici, 1997; Friel & Wainwright, 1998; Costa *et al*., 2000; Swan *et al*., 2003). These requirements seem to be reflected in the morphology of the jaws. Both trichiurids have elongate jaws [relative lengths with respect to cranial length of 0.76 (*T. lepturus*) and 0.85 (*A. carbo*)]. The presence of long jaws is also observed in other aquatic vertebrates and appears to be particularly effective for capturing mobile and elusive prey, and these predators rely on high-velocity jaw closure for capturing prey (Turingan & Wainwright, 1993; Norton & Brainerd, 1993; Ferry-Graham, Wainwright & Bellwood, 2001a; Ferry-Graham *et al*., 2001b; Porter & Motta, 2004; Kammerer *et al*., 2005). They are well suited for closing the tips of the jaws at high linear velocities but they have a mechanical disadvantage at their tips in terms of force production (Porter & Motta, 2004). Furthermore, long jaws increase gape size, allowing the animals to engulf or to seize relatively large prey between the jaws (Norton & Brainerd, 1993; Porter & Motta, 2004).

In previous research, the mechanical advantage of the mouth closing system has often been calculated in order to compare the ability of species with regards to mouth-closing velocity and biting capacity. Measured lengths of the in- and outlevers of the lower jaw enable lever ratios to be calculated, which gives some information about the force and velocity transmission or 'gearing' of the lower jaw: a large outlever relative to the inlever gives a high displacement advantage, while a relatively large inlever gives a high mechanical advantage. This relatively simple approach to the biomechanics of the lower jaw has proven to be valuable to predict differences in diet between species (Westneat, 1994; Turingan *et al*., 1995; Wainwright & Richard, 1995; Cutwa & Turingan, 2000).

However, the more detailed modelling presented here shows some limitations to this approach, in particular for fish with elongate jaws. First, our analysis shows that the forces resisting jaw closure (inertia, drag, pressure and tissue resistance) become more important in limiting the maximal speed of mouth closing in long-jawed trichiurids compared with, for example, the relatively shorter jaws of clariid catfishes (Van Wassenbergh *et al*., 2005). This implies that, during mouth closure, force transmission (and thus mechanical advantage) may also be important for building and maintaining velocity, and that this must also be considered along with the displacement advantage of the leverage system when evaluating jaw-closing performance. This is analogous to the situation in which we want to close an open door as quickly as possible: if the door is relatively long and heavy (a long, robust jaw), it is often advantageous to push the door at a point further away from the hinge (higher mechanical advantage) than it is to push near the hinge (high displacement or kinematic advantage). As a result, the power of the jaw muscles relative to the force-resistance to movement of the jaw is an important aspect in this process.

Yet, the results show that these trichiurid species still follow the traditional relationship between lever ratio and jaw closing performance when a jaw rotation is simulated from a gape angle of 50° to 10° (Fig. 10A). The acceleration phase, in which force transmission is important for increasing the angular velocity of the jaw, is limited to the first quarter of the total duration of this mouth closure. However, if we triple the length of the lower jaw of *T. lepturus* and simulate a 30–10° jaw rotation (which roughly approximates, for example, an extremely long jaw of a gar), the total duration (originally 0.166 s) becomes longer (0.203 s) if the inlever length is decreased by a factor of 0.8. This shows that we must be careful with the interpretation of lever ratios in relation to feeding performance in fishes with extremely elongated jaws (e.g. Kammerer *et al*., 2005).

The results of the present study also show that not only lever ratios, but also muscle inclination (Fig. 10C) and the aspect ratio of the muscle (Fig. 10B) are almost equally important factors in imposing the trade-off between biting and jaw closing performance. It can therefore be argued that further comparative research should, whenever possible, try to include these morphological variables as well (see also Westneat, 2004).

Adductor mandibulae complex

The ability of predators to bite hard depends on the isometric force generated by the jaw-adductor muscles, while the speed of jaw closure depends on

the shortening velocity of this muscle and how it is transmitted through the lever system (Barel, 1983; Westneat, 1994; Collar *et al.*, 2005). The teleost adductor mandibulae complex usually comprises different subdivisions. However, remarkably little information regarding potential independent actions of subdivisions on the lower jaw has been available. Yet, increased morphological complexity in jaw muscles (e.g. Tetraodontiformes, Loricarioidea) has been shown to be associated with increased functional complexity (Schaefer & Lauder, 1996; Friel & Wainwright, 1998, 1999; Korff & Wainwright, 2004).

Apart from some differences in the timing and the amount of force generated (Fig. 9), both trichiurid species show a similar pattern in the dynamic and static modelling results for the subdivisions of the mouth closing apparatus. However, comparing the model output between the different adductor mandibulae subdivisions, we see that the function of the individual subdivisions differs notably during mouth closing and biting (Fig. 8B).

The Aω subdivision has the largest PCSA and is the longest subdivision as well (Table 2). This subdivision generates considerable moment of force to accelerate the jaw rotation at the onset of jaw closing and remains the dominant subdivision to power mouth closure during the first half of mouth closure (Fig. 9). Owing to the force–length relationship and its elongation at wide gape angles, its position within the jaw system is probably less optimal to produce force at narrow gape angles. Still, the Aω clearly plays a dominant role in powering mouth closing, especially at the initial phase of mouth closing, where the A_1–A_2 and A_3 become suppressed (Fig. 9).

Because the Aω makes a relatively small angle with the inlever compared with the other subdivisions, the Aω limits the maximal gape of these two trichiurids. Interestingly, its configuration within the jaw system appears to be almost optimized for generating fast mouth closing if we assume that the mouth is opened up to an angle of about 50° during prey capture (Fig. 10). For producing high bite forces, the optimal inclination, for example, is much steeper (Fig. 10C). This may indicate that this muscle has evolved specifically to increase the speed of mouth closing.

Despite its smaller size compared with the Aω, the A_1–A_2 becomes the most important muscle at the moment of prey impact (Fig. 9). This muscle, and also the A_3, can operate rather constantly over a larger range of lower jaw angles compared with the Aω. The position of the A_1–A_2 in the jaw system is clearly a compromise between closing speed and static bite force. The design of the A_3 subdivision, by contrast, appears to be optimized for fast mouth closing as its performance in this task could not be improved by changing any of the morphological traits (Fig. 10).

These results indicate that the different parts of the adductor mandibulae complex could have evolved because of the different selective pressures to improve bite force or to improve the speed of jaw closing. The Aω apparently seems adapted for the role of a high-power jaw closing muscle, and is probably constrained in its configuration to preserve a sufficient gape size. The A_1–A_2 and A_3, by contrast, are better adapted to produce bite force over a wider range of gape angles and rotate the lower jaw at the instant of impact on the prey (Fig. 9). The discussion below gives an explanation for why none of the adductor subdivisions can be optimized for producing a powerful bite force (Fig. 10).

Streamlined head

Having a streamlined head shape allows aquatic animals to approach potential prey closely before striking. In addition, a streamlined head allows laminar flow of the surrounding water, even at higher swimming speeds (Porter & Motta, 2004). A consequent reduction of momentum generated on the water in front of the head (minimizing the bow wave) will reduce predator recognition by the prey. Trichiurid species typically approach their prey slowly (with a carangiform swimming pattern in *A. carbo* or an undulating dorsal fin in *T. lepturus*), the body held rigid (Bone, 1971). As prey fish are sensitive to size, shape and velocity of possible predators, the rigid body (reducing lateral undulatory movements) will reduce visual predator recognition by the prey (Porter & Motta, 2004). In addition, a slow approach (e.g. *Lepisosteus platyrhinus*) can be used to eliminate predator recognition by the prey (Porter & Motta, 2004).

Consequently, a streamlined head is advantageous for locomotion as well as for prey capture in fish. However, a streamlined head cannot always be combined with a jaw system optimized for producing large bite forces: Figure 10 shows that for both trichiurid species to exhibit maximal bite force (especially for the Aω), a conversion of the head configuration is required. In order to increase maximum bite force, an increase in input lever length and muscle inclination and a decrease in jaw muscle length are beneficial. An increase in maximal bite force may also be accomplished by jaw muscle hypertrophy, as observed in the clariid family (Van Wassenbergh *et al.*, 2005). As these morphological modifications make the head higher and broader, this may be disadvantageous for swimming (increase in drag), and optimizing streamlined head shape is therefore a trade-off with maximizing biting performance (Barel, 1983). This illustrates that trade-offs have to be considered not only within different aspect of feeding (biting and

closing the mouth), but also between feeding and locomotion if we fully want to understand the functional morphology of the jaw system in fishes.

ACKNOWLEDGEMENTS

We would like to thank K. E. Hartel of the Museum of Comparative Zoology (Harvard) for offering museum specimens. Research was partially funded by the FWO (G. 0388.00).

REFERENCES

Adams DC, Rohlf FJ. 2000. Ecological character displacement in *Plethodon*: biomechanical differences found from a geometric morphometric study. *Proceedings of the National Academy of Science of the United States of America* **97:** 4106–4111.

Anon. 2000. *Environment and biology of deep-water species Aphanopus carbo in NE Atlantic: basis for its management (BASBLACK)*. Final report of the EU study project 97/0084.

Barel CDN. 1983. Towards a constructional morphology of cichlid fishes (Teleostei, Perciformes). *Netherlands Journal of Zoology* **33:** 357–424.

Bock WJ, Shear ChR. 1972. A staining method for gross dissection of vertebrate muscles. *Anatomischer Anzeiger* **130:** 222–227.

Bone Q. 1971. On the scabbard fish *Aphanopus carbo*. *Journal of the Marine Biological Association UK* **51:** 219–225.

Bone Q, Marshall NB, Blaxter JHS. 1995. *Biology of fishes*, 2nd edn. London: Chapman & Hall.

Brainerd EL, Simons RS. 2000. Morphology and function of lateral hypaxial musculature in salamanders. *American Zoologist* **40:** 77–86.

Caroll AM, Wainwright PC, Huskey SH, Collar DC, Turinghan RG. 2004. Morphology predicts suction feeding performance in centrarchid fish. *Journal of Experimental Biology* **207:** 3873–3881.

Cheng CH, Kawasaki T, Hiang KP, Ho CH. 2001. Estimated distribution and movement of hairtail *Trichiurus lepturus* in the Aru Sea, based on the logbook records of trawlers. *Fisheries Science* **67:** 3–13.

Chiou WD, Chen CY, Wang CM, Chen CT. 2006. Food and feeding habits of ribbonfish *Trichiurus lepturus* in coastal waters of South-Western Taiwan. *Fisheries Science* **72:** 373–381.

Collar DC, Near TJ, Wainwright PC. 2005. Comparative analysis of morphological diversity: does disparity accumulate at the same rate in two lineages of centrarchid fishes? *Evolution* **59:** 1783–1794.

Costa G, Chubb JC, Veltkamp CJ. 2000. Cystacanths of *Bolbosoma vasculosum* in the black scabbard fish *Aphanopus carbo*, oceanic horse mackerel *Trachurus* and common dolphin *Delphinus delphis* from Madeira, Portugal. *Journal of Helminthology* **74:** 113–120.

Cutwa MM, Turingan RG. 2000. Intralocality variation in feeding biomechanics and prey use in *Archosargus probatocephalus* (Teleostei, Sparidae), with implications for the ecomorphology of fishes. *Environmental Biology of Fishes* **59:** 191–198.

Ferry-Graham LA, Wainwright PC, Bellwood DR. 2001a. Prey capture in long-jawed butterflyfishes (Chaetodontidae): the functional basis of novel feeding habits. *Journal of Experimental Marine Biology and Ecology* **256:** 167–184.

Ferry-Graham LA, Wainwright PC, Hulsey CD, Bellwood DR. 2001b. Evolution of mechanics of long jaws in Buterflyfishes (Family Chaetodontidae). *Journal of Morphology* **248:** 120–143.

Figueiredo I, Bordalo-Machado P, Reis S, Sena-Carvalho D, Blasdale T. 2003. Observations on the reproductive cycle of the black scabbardfish (*Aphanopus carbo* Lowe, 1839) in the NE Atlantic. *ICES Journal of Marine Science* **60:** 774–779.

Friel JP, Wainwright PC. 1998. Evolution of motor patterns in Teteraodontiform fishes: does muscle duplication lead to functional diversification? *Brain Behavior and Evolution* **52:** 159–170.

Friel JP, Wainwright PC. 1999. Evolution of complexity in motor patterns and jaw musculature of tetraodontiform fishes. *Journal of Experimental Biology* **202:** 867–880.

Gago FJ. 1998. Osteology and phylogeny of the cutlassfishes (Scombridae: Trichiuridae). *Contributions in Science* **476:** 1–79.

Hanken J, Wassersug R. 1981. The visible skeleton. A new double-stain technique reveals the native of the 'hard' tissues. *Functional Photography* **16:** 22–26.

Howe KM. 1979. First records of Oregon of the pelagic fishes *Paralepis atlantica, Gonostoma atlanticum, and Aphanopus carbo,* with notes on the anatomy of *Aphanopus carbo*. *Fishery Bulletin* **77:** 701–703.

Irschick DJ. 2002. Evolutionary approaches for studying functional morphology: examples from studies of performance capacity. *Integrative and Comparatice Biology* **42:** 278–290.

Kammerer CF, Grande L, Westneat MW. 2005. Comparative and developmental functional morphology of the jaws of living and fossil gars (Actinopterygii: Lepisosteidae). *Journal of Morphology* **267:** 1017–1031.

Korff WL, Wainwright PC. 2004. Motor pattern control for increasing crushing force in the striped burrfish (*Chilomycterus schoepfi*). *Zoology* **107:** 335–346.

Kwok KY, Ni IH. 2000. Age and growth of cutlassfishes, *Trichiurus spp*., from the South China Sea. *Fishery Bulletin* **98:** 748–758.

Liem KF. 1980. Acquisition of energy by teleosts: adaptive mechanisms and evolutionary patterns. In: Ali MA, ed. *Environmental physiology of fishes*. New York: Plenum Press, 299–334.

Liem KF, Osse JWM. 1975. Biological versatility, evolution, and food resources exploitation in African cichlid fishes. *American Zoologist* **15:** 427–454.

Losos JB, Walton BM, Bennett AF. 1993. Trade-offs

between sprinting and clinging ability in Kenyan chameleons. *Functional Ecology* **7:** 281–286.

Martins AS, Haimovici M. 1997. Distribution, abundance and biological interactions of the cutlassfish *Trichiurus lepturus* in the southern Brazil subtropical convergence ecosystem. *Fisheries Research* **30:** 217–227.

Mendez J, Keys A. 1960. Density and composition of mammalian muscle. *Metabolism* **9:** 184–188.

Nakamura I, Parin NV. 1993. Snake mackerels and cutlassfishes of the world (families Gempylidae and Trichiuridae). *FAO Fisheries Synopsis* **125:** 136.

Narici M. 1999. Human skeletal muscle architecture studied in vivo by non-evasive imaging techniques: functional significance and applications. *Journal of Electromyography and Kinesiology* **9:** 97–103.

Norton SF, Brainerd EL. 1993. Convergence in the feeding mechanics of ecomorphologically similar species in the Centrarchidae and Cichlidae. *Journal of Experimental Biology* **176:** 11–29.

Pasi BM, Carrier DR. 2003. Functional trade-offs in the limb muscles of dogs selected for running vs. fighting. *Journal of Evolutionary Biology* **16:** 541–541.

Pepin P, Koslow JA, Pearre S Jr. 1988. Labratory study of Foraging by Atlantic Mackerel, *Scomber scombrus*, on natural zooplankton Assemblages. *Fish Aquaculture* **45:** 879–887.

Porter HT, Motta PJ. 2004. A comparison of strike and prey capture kinematics of three species of piscivorous fishes: Florida gar (*Lepisosteus platyrhincus*), redfin needlefish (*Strongylura notata*), and great barracuda (*Sphyraena barracuda*). *Marine Biology* **145:** 989–1000.

Schaefer SA, Lauder GV. 1996. Testing historical hypotheses of morphological change: biomechanical decoupling in loricarioid catfishes. *Evolution* **50:** 1661–1675.

Schondube JE, del Rio CM. 2003. The flowerpiercers' hook: an experimental test of an evolutionary trade-off. *Proceedings of the Royal Society B Biological Sciences* **270:** 195–198.

Sibbing FA, Nagelkerke LAJ. 2001. Resource partitioning by Lake Tana barbs predicted from fish morphometrics and prey characteristics. *Reviews in Fish Biology and Fisheries* **10:** 393–437.

Stearns SC. 1992. *The evolution of life histories*. New York: Oxford University Press.

Studholme AL, Packer DB, Berrien PL, Johnson DL, Zetlin CA, Morse WW. 1999. Atlantic Mackerel, *Scomber scombrus*, life history and habitat characteristics. *NOAA Technical Memorandum NMFS-NE* **141:** 1–35.

Swan SC, Gordon JDM, Shimmield T. 2003. Preliminary investigations on the uses of otolith microchemistry for stock discrimination of the deep-water Black Scabbardfish (*Aphanopus carbo*) I the North East Atlantic. *Journal of the Northwest Atlantic Fishery Science* **31:** 221–231.

Tucker DW. 1956. Studies on the trichiuroid fishes – 3 A preliminary revision of the family Trichiuridae. *Bulletin of the British Museum of Natural History (Zoology)* **4:** 73–131.

Turingan RG, Wainwright PC. 1993. Morphological and functional bases of durophagy in the Queen Triggerfish, *Balistes vetula* (Pisces, Tetraodontiformes). *Journal of Morphology* **215:** 101–118.

Turingan RG, Wainwright PC, Hensley DA. 1995. Interpopulation variation in prey use and feeding biomechanics in Caribean Triggerfishes. *Oecologia* **102:** 296–304.

Van Leeuwen JL, Muller M. 1983. The recording and interpretation of pressures in prey-sucking fish. *Netherlands Journal of Zoology* **33:** 425–475.

Van Wassenbergh S, Aerts P, Adriaens D, Herrel A. 2005. A dynamical model of mouth closing movements in clariid catfishes: the role of enlarged jaw adductors. *Journal of Theoretical Biology* **234:** 49–65.

Wainwright PC, Richard BA. 1995. Predicting patterns of prey use from morphology of fishes. *Environmental Biology of Fishes* **44:** 97–113.

Westneat MW. 1994. Transmission of force and velocity in the feeding mechanisms of labrid fishes (Teleostei, Perciformes). *Zoomorphology* **114:** 103–118.

Westneat MW. 2004. Evolution of levers and linkages in the feeding mechanisms of fishes. *Integrative and Comparative Biology* **44:** 378–389.

Winterbottom R. 1974. A descriptive synonymy of the striated muscles of the Teleostei. *Proceedings of the Academy of Natural Sciences of Philadelphia* **125:** 225–317.

Wojciechowski J. 1972. Observations on the biology of cutlassfish *Trichiurus lepturus* L. (Trichiuridae) of Mauritania shelf. *Acta Ichthyologica et Piscatoria* **II:** 67–75.